

Land Cover Changes and Drivers in the Water Source Area of the Middle Route of the South-to-North Water Diversion Project in China from 2000 to 2015

GAO Wenwen¹, ZENG Yuan¹, ZHAO Dan¹, WU Bingfang¹, REN Zhiyuan²

(1. *State Key Laboratory of Remote Sensing Science, Institute of Remote Sensing and Digital Earth, Chinese Academy of Sciences, Beijing 100101, China*; 2. *Research Center for Policy and Technology of the Office of the South-to-North Water Diversion Project, Ministry of Water Resources, Beijing 100038, China*)

Abstract: The Middle Route of the South-to-North Water Diversion Project (MR-SNWDP) in China, with construction beginning in 2003, diverts water from Danjiangkou Reservoir to North China for residential, agriculture and industrial use. The water source area of the MR-SNWDP is the region that is most sensitive to and most affected by the construction of this water diversion project. In this study, we used Landsat Thematic Mapper (TM) and HJ-1A/B images from 2000 to 2015 by an object-based approach with a hierarchical classification method for mapping land cover in the water source area. The changes in land cover were illuminated by transfer matrixes, single dynamic degree, slope zones and fractional vegetation cover (FVC). The results indicated that the area of cropland decreased by 31% and was replaced mainly by shrub over the past 15 years, whereas forest and settlements showed continuous increases of 29.2% and 77.7%, respectively. The changes in cropland were obvious in all slope zones and decreased most remarkably (−43.8%) in the slope zone above 25°. Compared to the FVC of forest and shrub, significant improvement was exhibited in the FVC of grassland, with a growth rate of 16.6%. We concluded that local policies, including economic development, water conservation and immigration resulting from the construction of the MR-SNWDP, were the main drivers of land cover changes; notably, they stimulated the substantial and rapid expansion of settlements, doubled the wetlands and drove the transformation from cropland to settlements in immigration areas.

Keywords: remote sensing; land cover change; object-based classification; Middle Route of the South-to-North Water Diversion Project (MR-SNWDP); China

Citation: GAO Wenwen, ZENG Yuan, ZHAO Dan, WU Bingfang, REN Zhiyuan, 2020. Land Cover Changes and Drivers in the Water Source Area of the Middle Route of the South-to-North Water Diversion Project in China from 2000 to 2015. *Chinese Geographical Science*, 30(1): 115–126. <https://doi.org/10.1007/s11769-020-1099-y>

1 Introduction

Recently, many large-scale water diversion projects have been undertaken at the global level due to the disproportionate distribution of water resources in relation to rapid economic development. These projects have resulted in both economic benefits and adverse

eco-environmental effects (Boesch et al., 2001; Holland and Moore, 2003; Wang, 2004). China's South-to-North Water Diversion Project (SNWDP) is the world's largest water diversion project (Yao et al., 2019). The Middle Route of the South-to-North Water Diversion Project (MR-SNWDP) diverts water from Danjiangkou Reservoir along the Hanjiang River through the Yangtze

Received date: 2019-03-05; accepted date: 2019-07-01

Foundation item: Under the auspices of the National Key Research and Development Program of China (No. 2016YFC0500201-01), National Natural Science Foundation of China (No. 41671365, 41771464), the Annual Project of the Office of the South-to-North Water Diversion Project (No. 2018-21)

Corresponding author: ZENG Yuan. E-mail: zengyuan@radi.ac.cn

© Science Press, Northeast Institute of Geography and Agroecology, CAS and Springer-Verlag GmbH Germany, part of Springer Nature 2020

River, Huaihe River, Yellow River, Haihe River basins before finally arriving at Tuancheng Lake in Beijing. This project has transferred water to nearly 150 cities and 151 thousand ha of land through open channels, culverts and pipes (Miao et al., 2018; Kuo et al., 2019). Along the MR-SNWDP route, the water source area, including Danjiangkou Reservoir and the upper reaches of the Hanjiang River, plays a critical supportive role for this water source and has been greatly affected by the construction of the MR-SNWDP (Sheng and Webber et al., 2018).

Scholars have focused on significant changes in the eco-environment in the water source area of the MR-SNWDP. Dong et al. (2011) developed an improved watershed criterion model by establishing an accounting framework and method for computing payments for ecosystem services. Chen and Du (2008) described an evaluation of the potential ecological benefits and uses of the MR-SNWDP in short-term to long-term plans. Duan et al. (2012) defined and analysed extreme precipitation indices and found that extreme precipitation has become more frequent and had a higher intensity since the project began. Li and Zhang (2008) analysed the eco-environmental crisis and countermeasures for the water environment, land cover and soil erosion. Li et al. (2011) also assessed the spatial and temporal patterns of water quality and quantified natural and anthropogenic sources of water pollution using the FA-MLR receptor model. Tang et al. (2014) simulated the effects of pollutants on water quality to ensure that the water quality was maintained during the CR-SNWDP diversion process. Shen et al. (2013) studied land-use changes and their driving forces from 1990 to 2010 and concluded that the human factor exerted the main impact on the water source area of the MR-SNWDP. Zhou et al. (2012) analysed the fractional vegetation cover (FVC) in 2000 and 2009, and Li et al. (2009) monitored forest changes from 1980 to 2000. Above works monitored eco-environmental changes from many aspects, however, the drivers of these variations are lack in a comprehensive analysis in consideration of both the national and local influence.

Changes in land cover are significant indicators for environmental monitoring at the regional scale (Meyer and Turner, 1994; Veldkamp and Lambin, 2001; Lindquist et al., 2008; Berberoglu and Akin, 2009; Pouliot et al., 2009; Mao et al., 2018). Land cover

changes are crucial for assessing the effects of policies and decisions on land management and environmental protection (Pabi, 2007; Yan and Chen, 2013). Various methods have been successfully used for land cover classification, such as pixel-based approaches (Foody, 1996; Myint et al., 2011), object-based approaches (Burnett and Blaschke, 2003; Chen et al., 2009; Blaschke, 2010; Duro et al., 2012; Chen et al., 2012; Zhang et al., 2014a; Konik and Bradtke, 2016), and artificial neural networks (Kanellopoulos et al., 1992; Liu et al., 2004). FVC can be defined as the vertical projection of vegetation to the ground surface in a unit area (Kalle et al., 2007), which is an important auxiliary parameter to illustrate the drivers of land cover changes (Tømmervik et al., 2003; Wen et al., 2010; Jing et al., 2011). Although several works monitored land cover in this study area, a long-time-series analysis of land cover monitoring which started before the construction of the MR-SNWDP and ended after the official water supply, is still urgently needed.

In this study, we build a specific classification system and hierarchical decision tree using an object-based approach for land cover mapping and analysed the corresponding land cover changes and drivers based on transfer matrixes, single dynamic degree, slope zones and the FVC from 2000 to 2015. Based on land cover analysis in this study, we detected the spatial patterns and variations in land cover, and discussed the potential influence of land cover changes in two aspects, which included a series of local and national policies, to assess the effects of MR-SNWDP construction on the eco-environment.

2 Materials and Methods

2.1 Study area

The water source area of the MR-SNWDP is located between latitudes 31°20'N–34°10'N and longitudes 106°E–112°E. This area ranges over Shaanxi, Henan, Gansu, Sichuan, and Hubei provinces and Chongqing Municipality (Fig. 1); the catchment area is 94 500 km², and the catchment has a north subtropical monsoon climate. According to historical records, the mean annual precipitation and annual mean temperature are 873.3 mm and 13.71°C, respectively, and the flood season occurs from July to September (Wang and Ma, 1999).

The geomorphology consists of mountains, hills,

mounds and plains. From south to north, the area includes Shennongjia, Daba Mountain, Micang Mountain, the Qinling Mountains and Funiu Mountain and five primary plains (the Hanzhong Plain, Yunxian Plain, Junxian Plain, Nanyang Plain and Hanying-Ankang corridor). This area is characterized by a species-rich and multi-layered community of trees and is covered mainly by natural subtropical evergreen broadleaf, deciduous broadleaf and coniferous forests, as well as a mixture of these forest types. A heterogeneous vegetation distribution is obvious in this area and is characterized by high vegetation coverage in both the northern and southern mountainous areas and low vegetation coverage in the middle of the catchment.

2.2 Data and processing

We acquired 24 scenes (4 seasons) of Landsat TM (Thematic Mapper) data in 2000 and 12 scenes (2 sea-

sons) of HJ-1A/B data in 2010 and 2015 (Table 1). ASTER GDEM (Advanced space-borne thermal emission and reflection radiometer global digital elevation model) data with a 30-m resolution and 24-h daily precipitation data from 8 precipitation stations were used as ancillary data. We used parallel computing methods with supercomputers for the data pre-processing tasks, which included geometric correction, ortho-correction and topographic normalization. In addition, histogram equalization was conducted to reduce the spatial discontinuity among the different acquisition times.

In July of 2015, we collected 186 field samples (Fig. 1) based on stratified random sampling with the GVG (Global positioning system, GPS, Video and Geographic information system, GIS) app, which is commonly used for land cover observation at the regional scale by recording photos, locations and field attributes. A total of 2110 independently validated samples for the year 2000

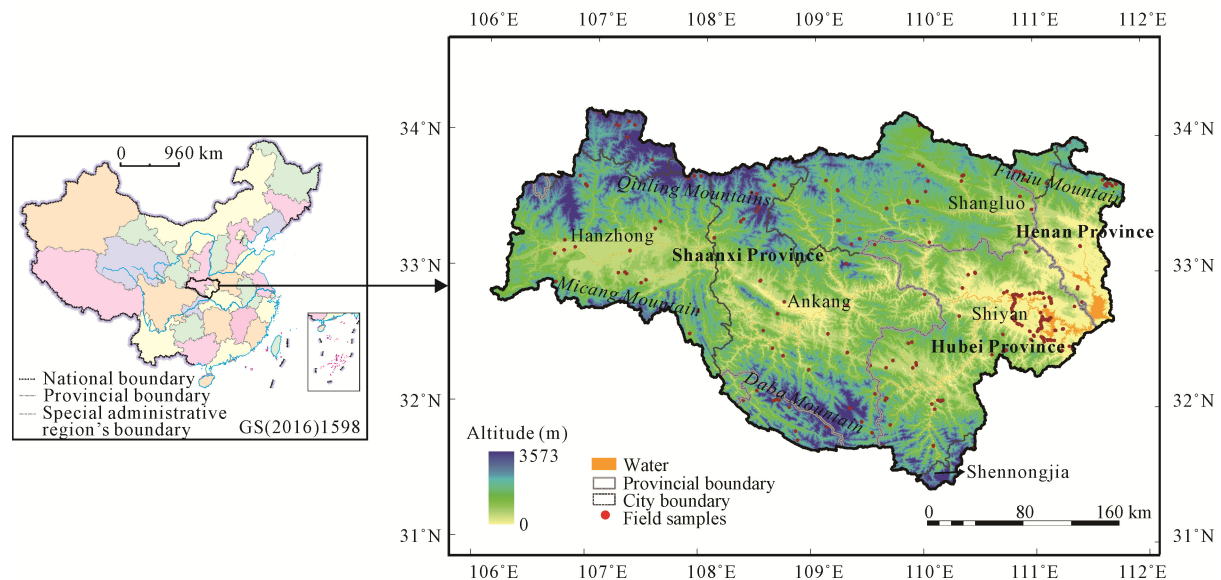


Fig. 1 Location of the study area and sampling sites

Table 1 Landsat Thematic Mapper (TM) and Huanjing (HJ)-1A/B images used in this study

Images	Year	Path/Row	Acquisition time (mon/d)	Images	Year	Path/Row	Acquisition time (mon/d)	Year	Path/Row	Acquisition time (mon/d)
Landsat TM	2010	125/037	3/11; 4/12; 7/17; 12/24	HJ-1A/B	2010	9/76	3/12	2015	3/76	2/11
		126/037	2/15; 5/5; 8/25; 12/15			8/76	3/10		9/76	3/28
		127/037	2/6; 4/26; 9/17; 11/20			11/76	4/28		5/76	5/19
		128/037	5/3; 5/19			6/76	4/28		12/76	7/28
		127/038	2/6; 5/12; 9/1; 11/4			5/76	6/17		9/76	8/21
		126/038	3/18; 5/5; 8/28			6/76	9/11		6/76	9/6
		125/038	4/12; 7/17; 12/24							

were selected from Google Earth. We also acquired 508 samples from the Worldview-2 images with a 0.5-m spatial resolution for 2010.

2.3 Land cover classification and accuracy assessment

The classification system used in this study conformed to the Land Cover Classification System (LCCS) of the Food and Agriculture Organization of the United Nations (FAO), with Level I classes including forest, shrub, grassland, wetlands, cropland, settlements and other land (Zhang et al., 2014a). An object-based approach was used for land cover classification, which started with the segmentation of the scales at multiple levels and generated objects as fundamental units (Desclee et al., 2006; Im et al., 2008; Cong et al., 2019). Then, a hierarchical classification was built and used five steps to separate 7 classes by analysing the sample features and empirical knowledge as follows (Zhang et al., 2014b; Wu et al., 2017). 1) The normalized difference vegetation index (NDWI) and the ratio vegetation index (RVI) were used to extract wetlands; 2) the normalized difference water index (NDVI) and the difference vegetation index (DVI) were used to distinguish natural vegetation and non-vegetation; 3) the NDVI combined with spectral features from January to March (before seeding) and June to August (growing) were used to extract cropland, during which time the geometric and texture features were used; 4) the spectral characteristics of the near-infrared and red bands were compared with those of the perpendicular vegetation index (PVI) to distinguish forest, shrub and grassland areas; and 5) the normalized difference built-up index (NDBI) (Kallel et al., 2007) combined with the NDVI and the geometric and texture features of the key features were employed to distinguish between settlements and other land. Then, the field samples were studied to revise these results. The above procedures were all performed in eCognition 8.0 software.

Kappa analysis based on a discrete multivariate approach was employed to verify the land cover accuracy (Congalton and Mead, 1983). The method generated the K statistic, which is a measure of consistency or precision between the remotely sensed classification and reference data.

2.4 Land cover change detection

In this study, transfer matrixes were used to quantitatively analyse the inner transformations between land cover types. The single dynamic degree of land cover was adopted to analyse land cover changes during different study periods. The method was defined as follows (Wang and Bao, 1999):

$$D_S = \frac{A_{t_2} - A_{t_1}}{A_{t_1}} \times \frac{1}{t_2 - t_1} \times 100\% \quad (1)$$

where A_{t_1} is the area of one land cover type in year t_1 and A_{t_2} is the area of the land cover type in year t_2 . Slope analysis was used to determine the distribution of land cover types and the characteristic trends of steep cropland (Table 2).

FVC is used to indicate vegetation growth and to detect drivers of land cover changes. In this study, we combined FVC with forest, shrub and grassland using a dimidiated pixel model. This model assumes that mixed pixel S can be described by S_{veg} to represent an all-vegetation ‘pure’ pixel, whereas S_{soil} represents a ‘pure’ soil pixel (Zhang et al., 2013). FVC is the proportion of vegetation cover in the pixel (f_c). Thus, a mixed pixel was derived as follows.

$$S = f_c \times S_{\text{veg}} + (1 - f_c) \times S_{\text{soil}} \quad (2)$$

The NDVI was notably correlated with the FVC. By inserting the NDVI into Eq. (2), we obtain the following approximation:

$$f_c = \frac{(NDVI - NDVI_{\text{soil}})}{(NDVI_{\text{veg}} - NDVI_{\text{soil}})} \quad (3)$$

where $NDVI_{\text{veg}}$ represents the vegetation pixels and $NDVI_{\text{soil}}$ represents the soil pixels. A cumulative frequency of 2% is taken as the $NDVI_{\text{soil}}$ value, and a cumulative frequency of 98% is taken as the $NDVI_{\text{veg}}$ value based on the NDVI data (Carlson and Ripley, 1997; Rundquist, 2002; Zhang et al., 2009).

Table 2 The area and proportion of the four slope zones in the water source area of the Middle Route of the South-to-North Water Diversion Project MR-SNWDP

Slope	<5°	5°–15°	15°–25°	>25°
Area (km ²)	6749	21571	31109	35090
Percentage (%)	7	23	33	37

3 Results

3.1 Land cover changes

Land cover changes in this area could be summarized as continuous decreases in cropland, grassland and other land. Wetlands and settlements continuously increased, and significant increases occurred in forest and decreases occurred in shrub from 2000 to 2015 (Fig. 2; Table 3). Forest was the main land cover type. The area increased by 12 853.2 km² from 2000 to 2010 but showed a small decrease of approximately 54.1 km² from 2010 to 2015. Cropland showed a considerable reduction of 3966.2 km² from 2000 to 2010 and then decreased slowly to 10 024.8 km² in 2015. Settlements increased continually during the 15-year period. Wetlands approximately doubled from 2000 to 2015. Other land, shrub and grassland all showed significant reductions from 2000 to 2010 but only slight changes from 2010 to 2015. The area of other land decreased obviously from 2000 to 2010 and then increased to 75.4 km² in 2015. The shrub area decreased notably by 6503 km² from 2000 to 2010 and then increased slightly by 128.2 km² from 2010 to 2015. Grassland decreased from 2000 to 2010 and then continued to decrease, with only a slight reduction of 142.2 km² occurring from 2010 to 2015.

The overall accuracy (OA) was 89.6% in 2000, 87.2% in 2010 and 84.4% in 2015, and the *K* statistic

was 87.5% in 2000, 83.8% in 2010 and 80.7% in 2015 (Table 4). Because of the high consistency within the remote sensing images and the large number of collected samples, the accuracy of the results was usually higher than that for the results based on field samples.

3.2 Transfer matrix

Based on the transfer matrix from 2000 to 2015 (Table 5), the increase in forest mainly came from shrub, with a change of 19 572 km², followed by the contributions of grassland, at 2207 km², and cropland, at 1949 km². In contrast, cropland showed a significant decrease and was mainly replaced by shrub, with 3475 km² and forest 1949 km². The area of shrub to forest transfer was 19 572 km², and that of grassland to shrub transfer was 3337 km².

3.3 Dynamic degree of land cover

During period 1 (2000 to 2010), the wetlands increased more rapidly than that of other land cover classes, with a dynamic degree of 77.5% (Table 6), followed by the increases for forest and settlements, with dynamic degrees of 29.8% and 27.0%, respectively. Other land decreased the most rapidly, with a dynamic degree of -74.0%, whereas the decreases in grassland, cropland, and shrub were -35.8%, -27.3%, and -25.1%, respectively. During period 2 (2010 to 2015), settlements

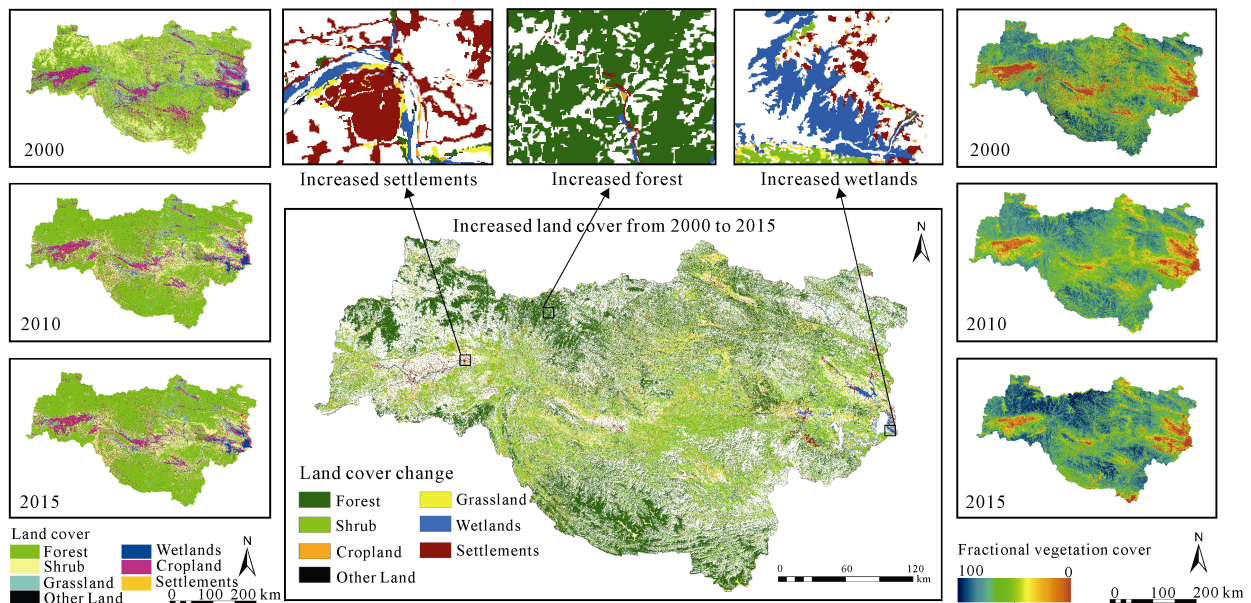


Fig. 2 Land cover mapping (left column), land cover changes (middle) and fractional vegetation cover (FVC) estimation (right column) for 2000, 2010 and 2015

Table 3 Land cover changes in 2000, 2010 and 2015 in the water source area of the MR-SNWDP (km²)

Land cover	2000	2010	2015	2000–2015
Forest	43131.7	55984.9	56039.0	12907.3
Shrub	25951.6	19448.6	19576.8	−6374.8
Grassland	8884.9	5707.1	5564.9	−3320.0
Wetlands	1092.9	1939.5	2130.3	1037.4
Cropland	14529.2	10563.0	10024.8	−4504.4
Settlements	608.8	773.3	1081.6	472.8
Other land	293.3	76.4	75.4	−217.9

Table 4 Accuracy of land cover in 2000, 2010 and 2015 (%)

Types	User accuracy		
	2000	2010	2015
Forest	94.6	90.5	88.9
Shrub	83.4	83.0	73.3
Grassland	87.6	81.1	71.4
Wetlands	94.3	90.3	88.9
Cropland	89.9	88.9	81.8
Settlements	90.1	85.4	93.3
Other land	82.7	75.0	71.4
<i>K</i>	87.5	83.8	80.7
Overall accuracy	89.6	87.2	84.4

increased significantly, with a dynamic degree of 39.9%, followed by wetlands, shrub and forest, with small increases in the dynamic degree of 9.8%, 0.7% and 0.1%, respectively. Cropland, other land and grassland decreased slowly, with dynamic degrees of −3.2%, −1.3% and −0.2%, respectively. Forest, shrub, grassland, wet-

lands, cropland and other land all varied significantly during period 1, followed by a slow rate of change during period 2.

3.4 Slope influence on land cover changes

The distribution of the seven land cover types in the four slope zones from 2000 to 2015 is shown in Fig. 3. In the slope zone below 5°, cropland occupied the largest proportion of the area at 54.7%, 42.9%, and 39.5% in 2000, 2010, and 2015, respectively. Forest and wetlands followed, whereas the proportion of settlements reached 10% and increased each year. In the zone from 5° to 15°, forest became the largest land cover component rather than cropland, and its proportions reached 41.3%, 42.9%, and 43.3% in 2000, 2010, and 2015, respectively. Shrub represented the second largest component, whereas wetlands and settlements showed a significant decrease, and the proportion of grassland increased significantly compared with that below the 5° zone. In the zone from 15° to 25°, forest was also the main land cover type, similar to the trend in the 5° to 15° zone, and the increase in the proportion of forest was greater than 15%, reaching 50.7%, 61.1%, and 61.0% in 2000, 2010, and 2015, respectively. In contrast, the proportion of cropland continually decreased, reaching 8.2% in 2015. In the zone above 25°, natural vegetation zones, including forest, shrub and grassland, accounted for more than 90% of the total area and increased from 2000 to 2015. Although cropland existed, its proportion decreased from 5.4% to 3.0%.

Table 5 Transfer matrix of land cover from 2000 to 2015 (km²)

Class	Forest	Shrub	Grassland	Wetlands	Cropland	Settlements	Other land	Total
Forest	31968	19572	2207	41	1949	80	37	55854
Shrub	7881	4659	3337	35	3475	102	10	19499
Grassland	1179	813	1758	45	1724	106	43	5668
Wetlands	239	172	144	871	549	26	119	2120
Cropland	1759	676	1357	74	6238	31	62	10197
Settlements	86	34	68	23	577	260	30	1078
Other land	16	12	11	4	17	3	12	75
Total	43128	25938	8882	1093	14529	608	313	94491

Table 6 Dynamic degree of land cover from 2000 to 2015 (%)

Period	Forest	Shrub	Grassland	Wetlands	Cropland	Settlements	Other land
1 (2000 to 2010)	29.8	−25.1	−35.8	77.5	−27.3	27.0	−74.0
2 (2010 to 2015)	0.1	0.7	−0.2	9.8	−3.2	39.9	−1.3

The slope analysis highlights detailed changes in forest and cropland (Fig. 4). Forest showed no obvious change in the slope zone below 15° , whereas in the slope zone above 15° , the area of forest increased notably from 2000 to 2010 and then became steady from 2010 to 2015. The changes in cropland from 2000 to 2015 were obvious in all slope zones. In each slope zone, cropland showed the same trend of decreasing quickly from 2000 to 2010 and then becoming stable within the next 5 yr. Cropland accounted for the largest area in the slope zone below 15° because frequent and intensive human activities were usually present in this zone. In the slope zone above 25° , cropland showed an obvious rate of decrease of 43.8%.

3.5 FVC influence on land cover changes

In this study, we combined land cover and FVC to estimate the quality of forest, shrub and grassland. From 2000 to 2015, the FVC values of these three land cover classes all increased at a rate of 17%. In particular, grassland increased from 0.38 in 2000 to 0.54 in 2015, with a growth rate of 16.6% (Table 7). According to the FVC of the field samples, the accuracy was $R^2 = 0.8161$ in 2010 (Zhou et al., 2012) and $R^2 = 0.7894$ in 2015 based on 17 collected field samples (Fig. 5).

In this study, the FVC was stratified as follows: $FVC > 0.8$, $0.6 < FVC < 0.8$, $0.3 < FVC < 0.6$ and $FVC < 0.3$. We analysed the changes in the proportions of FVC classes, in which the variation in area could be ignored (Fig. 6). For forest, the FVC values were mainly greater than 0.6. The proportion of areas with FVC values over 0.6 in 2000 was 71.6%, after which time the proportion increased significantly to 90.1% in 2010 and 97.1% in 2015. For areas with FVC values below 0.3, the proportion decreased from 7.5% in 2000 to 0.9% in 2015. The areas with FVC values of shrub were concentrated above 0.6. The proportions of areas with FVC values over 0.6 were 71.0% in 2000 and 72.2% in 2010, and the proportion increased significantly to 84.2% in 2015. For areas with FVC values below 0.3, the proportion was only 6.5% in 2000 and then decreased sharply to 1.9% in 2010 and 1.3% in 2015. For grassland, the primary FVC values ranged from 0.3 to 0.8. The proportions of areas with FVC values ranging from 0.3 to 0.8 were 56.3% in 2000 and then increased greatly to 67.2% in 2015. An obvious increase in the FVC values occurred from 2000 to 2010. For areas with FVC values below 0.3, the proportion was 33.6% in 2000, decreased to 10.4% in 2010 and was only 6.0% in 2015. The increase in FVC marked significant

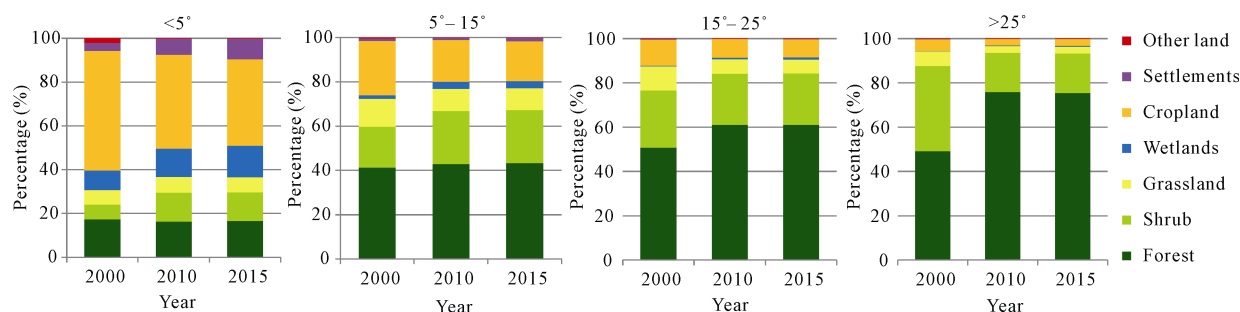


Fig. 3 Proportions of land cover in the different slope zones from 2000 to 2015

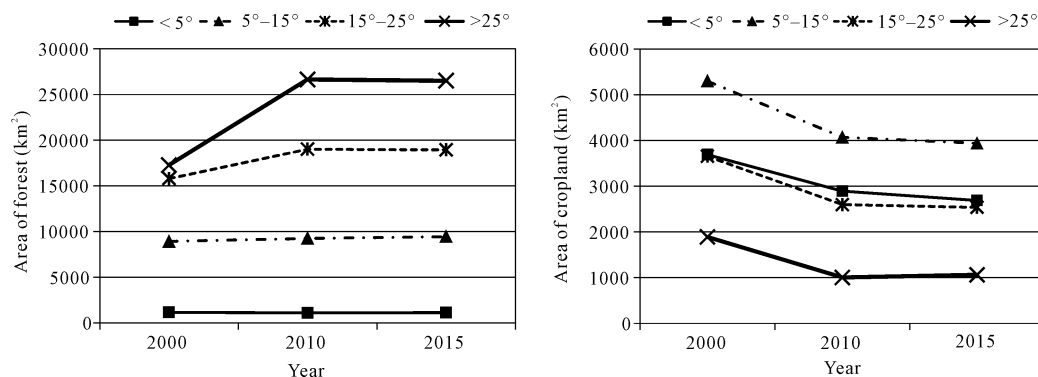


Fig. 4 Trends of forest (left) and cropland (right) in the different slope zones from 2000 to 2015

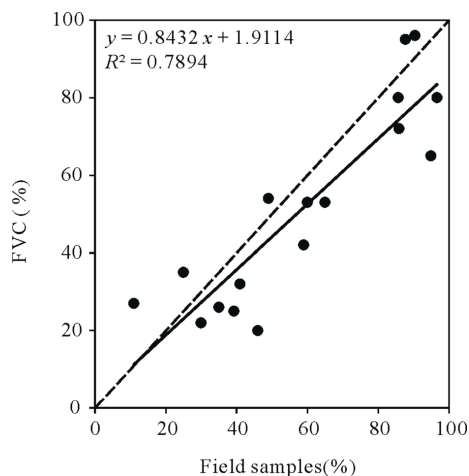


Fig. 5 Accuracy of fractional vegetation cover (FVC) by remote sensing in 2015

changes in vegetation. As shown in this study, the FVC values of forest, shrub and grassland all increased during

the 15-year period, with growth rates of 14.9%, 2.98%, and 16.6% in 2000, 2010, and 2015, respectively.

4 Discussion

This study presents multiple changes in land cover in the water source area of the MR-SNWDP, which have been influenced mainly by both national and local policies (Fig. 7). After floods occurred in the Yangtze and Songhua River basins in 1998, the government began to rectify past damage to the natural ecosystem and then

Table 7 Fractional vegetation cover (FVC) values of forest, shrub and grassland from 2000 to 2015

FVC	2000	2010	2015
Forest	0.67	0.75	0.77
Shrub	0.67	0.65	0.69
Grassland	0.38	0.51	0.54

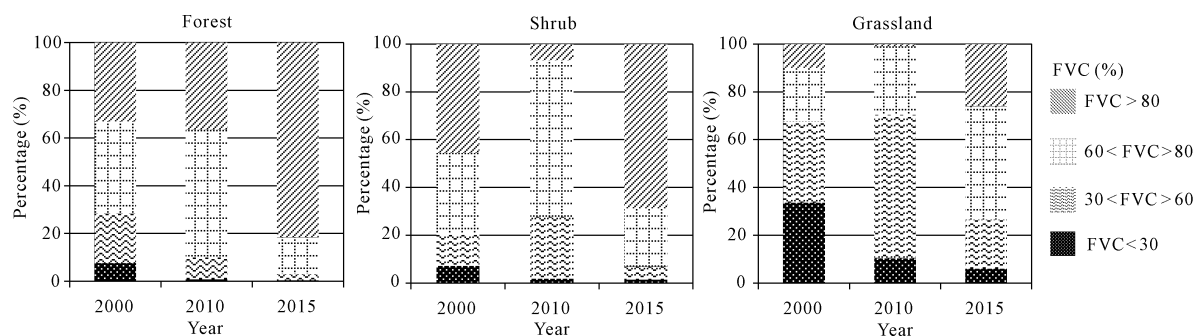


Fig. 6 The distribution of fractional vegetation cover (FVC) values for forest, shrub and grassland from 2000 to 2015

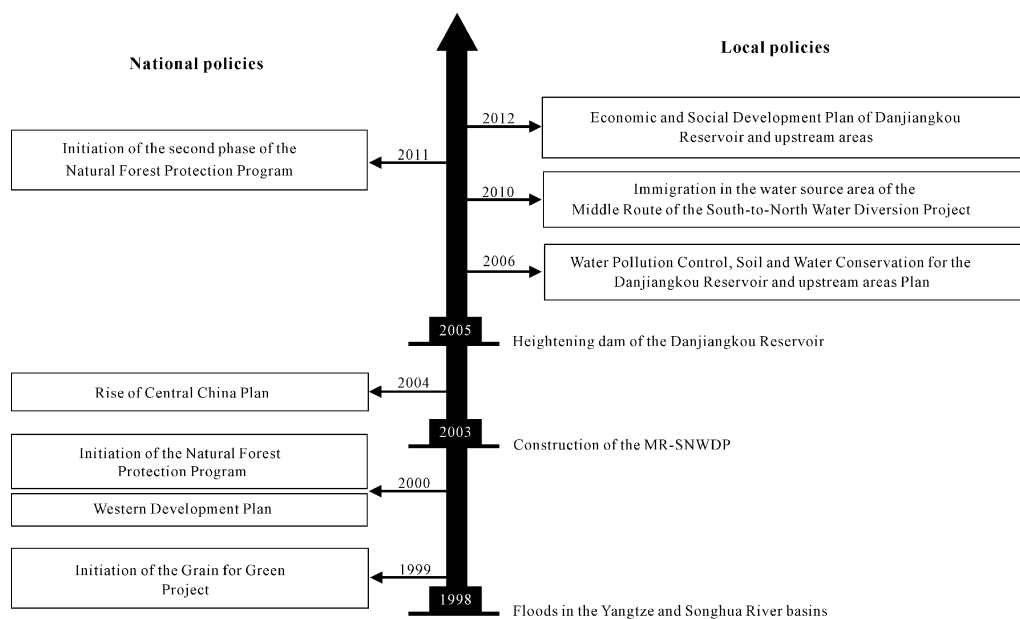


Fig. 7 Key events affecting land cover changes from 1998–2015

implemented the Grain for Green Project in 1999 (GGP), Natural Forest Protection (NFP) in 2000 and a series of economic development plans, including the Western Development Plan in 2000 and Rise of Central China Plan in 2004. The GGP aimed to relieve soil erosion and land desertification (Ouyang, 2007; Chi et al., 2019). Cropland changes in steep slopes were reduced. In the slope zone above 25° , the rate of decrease reached 43.8%, resulting in the restoration of 826 km² to natural vegetation from 2000 to 2010. The NFP aims to limit the felling of trees and rehabilitate the vegetation growing in the main natural forest area (Feng and Chen, 2009), which have promoted the transformation from shrub to forest and from grassland to shrub. After achieving excellent effects by expansion of natural vegetation during its first 10 years, the NFP implemented its second phase in 2011 (Gao et al., 2007). Therefore, the FVC of forest, shrub and grassland all increased during the 15-year period, with growth rates of 14.9%, 2.98%, and 16.6%, respectively. However, the characteristic changes in land cover in this study area were mainly affected by local policies caused by the construction of the MR-SNWDP.

MR-SNWDP construction started in 2003. Because of the special water supply function in this region, several local conservation and economic development policies have been established. For instance, the Water Pollution Control, Soil and Water Conservation Plan implemented and government focused on vegetation quality, such as consolidating achievement, water conservation and standardized management. The increase in the FVC marked significant changes in vegetation under this policy. As shown in this study, the forest coverage rate increased from 45.6% (2000) to 59.3% (2015) as a result of the afforestation of cropland and other land. The proportion of forest with FVC values over 0.6 increased significantly, and that with FVC below 0.3 decreased from 7.5% in 2000 to 0.9% in 2015. The increased FVC has improved not only water and soil conservation (Gu et al., 2013) but also carbon sequestration, the accumulation of vegetation nutrients, air purification, forest protection and the maintenance of biological diversity. The high-density forest, shrub and grassland can form a protective layer to prevent areas with a slope above 15° from weathering and mitigate raindrops hitting the soil directly under concentrated heavy rain (Jian et al., 2015; Li et al., 2016). These vegetation types ef-

fectively intercept surface runoff, which weakens the erosion ability and prevents the occurrence of rill or gully erosion (Wang et al., 2017).

The Economic and Social Development Plan improved the regional economy and immediately stimulated the development of the gross domestic product (GDP), which showed an obvious increase from 185.9 billion yuan (RMB) in 2010 to 373.3 billion yuan (RMB) in 2015 (National Bureau of Statistics, 2010). The GDP growth rate from 2010 to 2015 was more than twice that in the first ten years (Fig. 8). These economic developments spurred the substantial expansion of settlements (Azadi et al., 2011) and rapid settlement expansion, which resulted in a higher dynamic degree of settlements from 2010 to 2015 than from 2000 to 2010. Throughout the study period, the increased demands for food, housing, working environments, industrial buildings, and transportation facilities, as well as job opportunities, positively impacted cropland construction and while correspondingly accelerated the regional economy (Kuang et al., 2016).

In addition, the immigration plan started in 2010. The related population was approximately 345 thousand individuals, and nearly two-thirds of the immigrants required relocation to 16 new towns, which were almost all located in mountainous areas (Kuo et al., 2019). Construction in mountainous settlements may destroy the original vegetation, whereas construction in the plains occupies cropland and bare land. The immigrants felled trees for construction, leading to the transformation of forests into shrub and grassland, especially in areas with high population densities. Thus, this policy led to a small decrease in forest and a significant increase in settlements and wetlands from 2010 to 2015. Moreover, the policy resulted in a high percentage of the

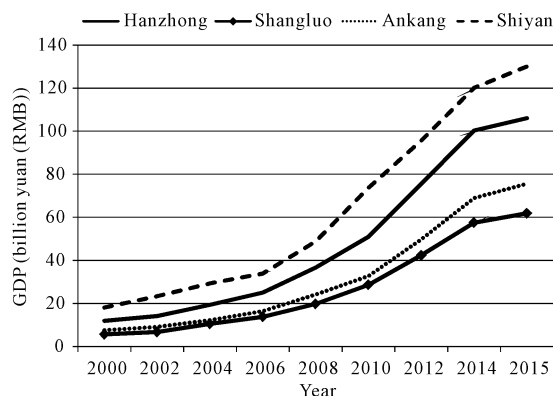


Fig. 8 Gross domestic products (GDP) of the four main cities in

study area from 2000 to 2015

agricultural population in mountain regions immigrating to cities and counties, which contributed to the transformation of cropland to fallow land.

Furthermore, the Danjiangkou Reservoir dam increased in height from 162 to 176.6 m, which increased the water level during the construction period and flooded a large area, involving 6 counties, 40 towns and 441 villages in Henan and Hubei Provinces. Therefore, the area of wetlands approximately doubled from 2000 to 2015.

5 Conclusions

In contrast to previous related studies in the area of the MR-SNWDP, this study mapped long-term series of land cover and performed a comprehensive analysis of land cover changes. An obvious increasing trend was found for forest, with an increase (12 853.2 km²) from 2000 and 2010 but a slight decrease (54.1 km²) from 2010 to 2015. Cropland, other land, shrub and grassland all showed significant reductions over the 15-year study period. Settlements increased continually, and wetlands approximately doubled. Forest displayed the largest area in the slope zone above 15°, whereas cropland presented the largest area in the slope zone below 15°. In the slope zone above 25°, cropland decreased greatly (−43.8%). In addition, obvious improvement in the density of natural vegetation was shown by the increasing FVC of forest, shrub and grassland.

In this study, changes in land cover can indicate variations in the ecological environment, which have been mainly influenced by both national and local policies. With rapid social and economic development, the adoption of strict water conservation measures is urgently needed. Remote sensing techniques have been broadly applied in the ecological research field. Based on time series of ecological parameters estimated with in situ data, such as land cover, FVC, leaf area index, and net primary productivity data, new methods for eco-environmental assessment at regional and even national scales can be developed. However, the coordination of ecological requirements and remote sensing abilities becomes a key problem under such scenarios. The analysis scale and scaling issues largely limit the multi-scale advantages of remote sensing data, reflecting the complexity of ecological processes. Determining

how to assess the ecological service functions of various ecosystems and proposing a systematic methodology combined with ecology and remote sensing techniques require extensive research. In the water source area of the MR-SNWDP, water quality is receiving increasing attention because this water is now being delivered to North China. Therefore, the continuous monitoring of land cover changes by up-to-date remote sensing techniques is highly required in this area.

Acknowledgements

We gratitude the project cooperation from Wang Zhimin, Liu Yuanshu, Cao Pengfei, Hou Kun, Meng Lingguang, Hu Guiquan. We also thank Zhao Yujin, Zheng Zhaoju, Dong Wenxue, and Yi Haiyan for their assistance in the field sample collection.

References

- Azadi H, Ho P, Hasfiati L, 2011. Agricultural land conversion drivers: a comparison between less developed, developing and developed countries. *Land Degradation and Development*, 22(6): 596–604. doi: 10.1002/ldr.1037
- Berberoglu S, Akin A, 2009. Assessing different remote sensing techniques to detect land use/cover changes in the eastern Mediterranean. *International Journal of Applied Earth Observation and Geoinformation*, 11(1): 46–53. doi: 10.1016/j.jag.2008.06.002
- Blaschke T, 2010. Object based image analysis for remote sensing. *Journal of Photogrammetry and Remote Sensing*, 65(1): 2–16. doi: 10.1016/j.isprsjprs.2009.06.004
- Boesch D F, Burroughs R H, Baker J E et al., 2001. *Marine Pollution in the United States*. Pew Oceans Commission, Arlington, Virginia
- Burnett C, Blaschke T, 2003. A multi-scale segmentation/object relationship modelling methodology for landscape analysis. *Ecological Modelling*, 168(3): 233–249. doi: 10.1016/S0304-3800(03)00139-X
- Carlson T N, Ripley D A, 1997. On the relation between NDVI, fractional vegetation cover, and leaf area index. *Remote Sensing of Environment*, 62: 241–252. doi: 10.1016/S0034-4257(97)00104-1
- Chen G, Hay G J, Carvalho L M T et al., 2012. Object-based change detection. *International Journal of Remote Sensing*, 33: 4434–4457. doi: 10.1080/01431161.2011.648285
- Chen H C, Du P F, 2008. Potential Ecological Benefits of the Middle Route for the South-North Water Diversion Project. *Tsinghua Science and Technology*, 13(5): 715–719. doi: 10.1016/S1007-0214(08)70116-0
- Chen Y H, Su W, Li J et al., 2009. Hierarchical object oriented classification using very high resolution imagery and LIDAR

- data over urban areas. *Advances in Space Research*, 43: 1101–1110. doi: 10.1016/j.asr.2008.11.008
- Chi W F, Zhao Y Y, Kuang W H et al., 2019. Impacts of anthropogenic land use/cover changes on soil wind erosion in China. *Science of The Total Environment*, 668: 204–215. doi: 10.1016/j.scitotenv.2019.03.015
- Cong Pifu, Chen Kexin, Qu Limei et al., 2019. Dynamic Changes in the Wetland Landscape Pattern of the Yellow River Delta from 1976 to 2016 Based on Satellite Data. *Chinese Geographical Science*, 29(3): 372–381. doi: 10.1007/s11769-019-1039-x
- Congalton R G, Mead R A, 1983. A Quantitative Method to Test for Consistency and Correctness in Photointerpretation. *Photogrammetric Engineering & Remote Sensing*, 49(1): 69–74.
- Desclée B, Bogaert P, Defourny P, 2006. Forest change detection by statistical object-based method. *Remote Sensing of Environment*, 102(1-2): 1–11. doi: 10.1016/j.rse.2006.01.013
- Dong Z J, Yan Y, Duan J et al., 2011. Computing payment for ecosystem services in watersheds: an analysis of the Middle Route Project of South-to-North Water Diversion in China. *Journal of Environmental Sciences*, 23(12): 2005–2012. doi: 10.1016/S1001-0742(10)60663-8
- Duan Z R, Zhang L P, Li L C, 2012. The Extreme Precipitation Change Characteristics of the Source Area of the Middle Route of South-North Water Transfer Project. *Procedia Engineering*, 28: 569–573. doi: 10.1016/j.proeng.2012.01.770
- Duro D C, Franklin S E, DubéMG, 2012. A comparison of pixel-based and object-based image analysis with selected machine learning algorithms for the classification of agricultural landscapes using SPOT-5 HRG imagery. *Remote Sensing of Environment*, 118: 2–16. doi: 10.1016/j.rse.2011.11.020
- Feng Qinliang, Chen Jiancheng, 2009. Sustainable Development of Natural Forest Protection Project Area. *Journal of Beijing Forestry University (Social Sciences)*, 8(4): 28–31. (in Chinese)
- Foody G M, 1996. Approaches for the production and evaluation of fuzzy land cover classifications from remotely sensed data. *International Journal of Remote Sensing*, 17(7): 1317–1340. doi: 10.1080/01431169608948706
- Gao Guoxiong, Zhang Guoliang, Liu Meixian et al., 2007. Retrospect on the research and practice of the converting cropland to forests. *Journal of Northwest Forestry University*, 22(2): 203–208. (in Chinese)
- Gu Z J, Wu X X, Zhou F et al., 2013. Estimating the effect of pinus massoniana Lamb plots on soil and water conservation during rainfall events using vegetation fractional coverage. *Catena*, 109: 225–233. doi: 10.1016/j.catena.2013.03.008
- Holland S P, Moore M R, 2003. Cadillac desert revisited: property rights, public policy, and water-resource depletion. *Journal of Environmental Economics and Management*, 46(1): 131–155. doi: 10.1016/S0095-0696(02)00036-0
- Im J, Jensen J R, Hodgson M E, 2008. Object-based land cover classification using high-posting-density lidar data. *GIScience and Remote Sensing*, 45(2): 209–228. doi: 10.2747/1548-1603.45.2.209
- Jian S Q, Zhao C Y, Fang S M et al., 2015. Effects of different vegetation restoration on soil water storage and water balance in the Chinese Loess Plateau. *Agricultural and Forest Meteorology*, 206: 85–96. doi: 10.1016/j.agrformet.2015.03.009
- Jing X, Yao W Q, Wang J H et al., 2011. A study on the relationship between dynamic change of vegetation Coverage and precipitation in Beijing's mountainous areas during the last 20 years. *Mathematical and Computer Modelling*, 54(3-4): 1079–1085. doi: 10.1016/j.mcm.2010.11.038
- Kallel A, Le Hégarat-Masclé S, Otlé C et al., 2007. Determination of vegetation cover fraction by inversion of a four-parameter model based on isoline parametrization. *Remote Sensing of Environment*, 111(4): 553–566. doi: 10.1016/j.rse.2007.04.006
- Kanellopoulos I, Varfis A, Wilkinson G G et al., 1992. Land-cover discrimination in SPOT HRV imagery using an artificial neural network—a 20-class experiment. *International Journal of Remote Sensing*, 13(5): 917–924. doi: 10.1080/01431169208904164
- Konik M, Bradtke K, 2016. Object-oriented approach to oil spill detection using ENVISAT ASAR images. *Journal of Photogrammetry and Remote Sensing*, 118: 37–52. doi: 10.1016/j.isprsjprs.2016.04.006
- Kuang W H, Liu J Y, Dong J W et al., 2016. The rapid and massive urban and industrial land expansions in China between 1990 and 2010: a CLUD-based analysis of their trajectories, patterns, and drivers. *Landscape and Urban Planning*, 145: 21–33. doi: 10.1016/j.landurbplan.2015.10.001
- Kuo Y M, Liu W W, Zhao E M et al., 2019. Water quality variability in the middle and down streams of Han River under the influence of the Middle Route of South-North Water diversion project, China. *Journal of Hydrology*, 569: 218–229. doi: 10.1016/j.jhydrol.2018.12.001
- Li Lu, Shi Zhihua, Zhu Dun et al., 2009. Forest Changes in the Water Source Area of Middle Route of the South-to-North Water Diversion Project. *Journal of Natural Resources*, 24(6): 1049–1057. (in Chinese)
- Li S, Liang W, Fu, B J et al., 2016. Vegetation changes in recent large-scale ecological restoration projects and subsequent impact on water resources in China's Loess Plateau. *Science of the Total Environment*, 569–570: 1032–1039. doi: 10.1016/j.scitotenv.2016.06.141
- Li Siyue, Zhang Quanfa, 2008. Main Eco-Environmental Problems and Revegetation in the Danjiangkou Reservoir Water Supplying Area of the Middle Route of the South to North Water Transfer Project. *China Rural Water and Hydropower*, (3): 1–4. (in Chinese)
- Li S Y, Li J, Zhang Q F, 2011. Water quality assessment in the rivers along the water conveyance system of the Middle Route of the South to North Water Transfer Project (China) using multivariate statistical techniques and receptor modeling. *Journal of Hazardous Materials*, 195: 306–317. doi: 10.1016/j.jhazmat.2011.08.043
- Lindquist E J, Hansen M C, Roy D P et al., 2008. The suitability of decadal image data sets for mapping tropical forest cover change in the Democratic Republic of Congo: implications for the global land survey. *International Journal of Remote Sensing*

- ing, 29(24): 7269–7275. doi: 10.1080/01431160802275890
- Liu Z J, Liu A X, Wang C Y et al., 2004. Evolving neural network using real coded genetic algorithm (GA) for multispectral image classification. *Future Generation Computer Systems*, 20(7): 1119–1129. doi: 10.1016/j.future.2003.11.024
- Mao D H, Wang Z M, Wu J G et al., 2018. China's wetlands loss to urban expansion. *Land Degradation and Development*, 29(8): 2644–2657. doi: 10.1002/ldr.2939.
- Meyer W B, Turner B L, 1994. *Changes in Land Use and Land Cover: A Global Perspective*. Cambridge, UK: Cambridge University Press.
- Miao Z, Sheng J C, Webber M et al., 2018. Measuring water use performance in the cities along China's South-North Water Transfer Project. *Applied Geography*, 98: 184–200. doi: 10.1016/j.apgeog.2018.07.020
- Myint S W, Gober P, Brazel A et al., 2011. Per-pixel vs. object-based classification of urban land cover extraction using high spatial resolution imagery. *Remote Sensing of Environment*, 115(5): 1145–1161. doi: 10.1016/j.rse.2010.12.017
- M Konik, K Bradtke. Object-oriented approach to oil spill detection using ENVISAT ASAR images. *Journal of Photogrammetry and Remote Sensing*, 118: 37–52. doi: 10.1016/j.isprsjprs.2016.04.006
- National Bureau of Statistics. 2010. *China Statistical Yearbook*. Beijing: China Statistics Press.
- Ouyang Zhiyun, 2007. *Ecological Construction and Sustainable Development in China*. Beijing: Science Press. (in Chinese)
- Pabi O, 2007. Understanding land-use/cover change process for land and environmental resources use management policy in Ghana. *Geojournal*, 68(4): 369–383. doi: 10.1007/s10708-007-9090-z
- Pouliot D, Latifovic R, Olthof I, 2009. Trends in vegetation NDVI from 1 km AVHRR data over Canada for the period 1985–2006. *International Journal of Remote Sensing*, 30(1): 149–168. doi: 10.1080/01431160802302090
- Rundquist B C, 2002. The influence of canopy green vegetation fraction on spectral measurements over native tall-grass prairie. *Remote Sensing of Environment*, 81(1): 129–135. doi: 10.1016/S0034-4257(01)00339-X
- Shen Huaifei, Hou Gang, Zhai Shumei et al., 2013. Land Use/Cover Change and the Driving Force in the Water Supplying Area of the Middle-Route of the South-to-North Water Diversion (MR-SNWD) Project. *Guizhou Agricultural Sciences*, 41(6): 167–171. (in Chinese)
- Sheng J C, Webber M, 2018. Using incentives to coordinate responses to a system of payments for watershed services: the middle route of South-North Water Transfer Project, China. *Ecosystem Services*, 32: 1–8. doi: 10.1016/j.ecoser.2018.05.005
- Tømmervik H, Høgda J A, Solheim I, 2003. Monitoring vegetation changes in Pasvik (Norway) and Pechenga in Kola Peninsula (Russia) using multitemporal Landsat MSS/TM data. *Remote Sensing of Environment*, 85(3): 370–388. doi: 10.1016/S0034-4257(03)00014-2
- Tang C H, Yi Y J, Yang Z F et al., 2014. Water pollution risk simulation and prediction in the main canal of the South-to-North Water Transfer Project. *Journal of Hydrology*, 519: 2111–2120. doi: 10.1016/j.jhydrol.2014.10.010
- Veldkamp A, Lambin E F, 2001. Predicting land-use change. *Agriculture, Ecosystems and Environment*, 85(1–3): 1–6. doi: 10.1016/S0167-8809(01)00199-2
- Wang Fang, Ge Quansheng, Yu Qibiao et al. 2017. Impacts of Land-use and Land-cover Changes on River Runoff in Yellow River Basin for Period of 1956–2012. *Chinese Geographical Science*, 27(1): 13–24. doi: 10.1007/s11769-017-0843-3
- Wang L S, Ma C, 1999. A study on the environmental geology of the Middle Route Project of the South-North water transfer. *Engineering Geology*, 51: 153–165.
- Wang Xiuli, 2004. The famous water transfer project in the basin and districts aboard. *Water Resources and Electric Power*, 30(1): 1–25. (in Chinese)
- Wang Xiulan, Bao Yuhai, 1999. Study on the methods of land use dynamic change research. *Progress in Geography*, 18(1): 81–87. (in Chinese).
- Wen Z M, Lees B G, Jiao Feng et al., 2010. Stratified vegetation cover index: a new way to assess vegetation impact on soil erosion. *Catena*, 83(1): 87–93. doi: 10.1016/j.catena.2010.07.006
- Wu Bingfang et al., 2017. *Land Cover Atlas of the People's Republic of China (1:1,000,000)*. Sinomaps Press.
- Yan B W, Chen L, 2013. Coincidence probability of precipitation for the middle route of South-to-North water transfer project in China. *Journal of Hydrology*, 499: 19–26. doi: 10.1016/j.jhydrol.2013.06.040
- Yao Y Y, Zheng C M, Andrews C et al., 2019. Integration of groundwater into China's south-north water transfer strategy. *Science of The Total Environment*, 658: 550–557. doi: 10.1016/j.scitotenv.2018.12.185
- Zhang J X, Liu Z J, Sun X X, 2009. Changing landscape in the Three Gorges Reservoir Area of Yangtze River from 1977 to 2005: land use/land cover, vegetation cover changes estimated using multi-source satellite data. *International Journal of Applied Earth Observation and Geoinformation*, 11(6): 403–412. doi: 10.1016/j.jag.2009.07.004
- Zhang L, Jia K, Li X S et al., 2014a. Multi-scale segmentation approach for object-based land-cover classification using high-resolution imagery. *Remote Sensing Letters*, 5(1): 73–82. doi: 10.1080/2150704X.2013.875235
- Zhang L, Li X S, Yuan Q Z et al., 2014b. Object-based approach to national land cover mapping using HJ satellite imagery. *Journal of Applied Remote Sensing*, 8: 083686. doi: 10.1117/1.JRS.8.083686
- Zhang X F, Liao C H, Li J H et al., 2013. Fractional vegetation cover estimation in arid and semi-arid environments using HJ-1 satellite hyperspectral data. *International Journal of Applied Earth Observation and Geoinformation*, 21: 506–512. doi: 10.1016/j.jag.2012.07.003.
- Zhou Zhiqiang, Zeng Yuan, Zhang Lei et al., 2012. Remote Sensing Monitoring and Analysis of Fractional Vegetation Cover in the Water Source Area of the Middle Route of Projects to Divert Water from the South to the North. *Remote Sensing For Land & Resources*, 24(1): 70–76. (in Chinese)